Journal of Engineering Science and Technology
Vol. 13, No. 6 (2018) 1834 - 1849


# A PROPOSED REFERENCE CURRENT SIGNAL GENERATION TECHNIQUE FOR SHUNT ACTIVE POWER FILTER

B. NAYAK, B. MISRA*, A. MOHAPATRA

School of Electrical Engineering, KIIT University, Bhubaneswar-24, India
*Corresponding Author: bmisrafel@kiit.ac.in

**Abstract**

This paper presents a new control technique for reference current generation for shunt active power filter to eliminate harmonics and to compensate the reactive power required by non-linear load using adaptive hysteresis band control. Two-phase lock loop (PLL) controllers are utilised here to extract the phase angles of distorted load side current and source voltage. The normalisation and delay-signal cancellation techniques are utilized to extract the positive sequence of distorted signals, which is necessary to get the accurate information of phase angle. The peak current magnitude and the phase angle information of signals are used to generate the appropriate signals for the reference current. The adaptive hysteresis band controller, proposed in the literature is adopted here to generate the constant frequency switching pulses for the firing of 6-active switches of the inverter. The capacitor voltage is maintained constant through a voltage feedback utilising PI controller. The performance of the new active power filter (APF) is evaluated in MATLAB/Simulink power system toolbox. Simulation study provides quite satisfactory results for the elimination of harmonics and compensation of reactive power of the utility grid current under different load conditions. The total harmonic distortion (THD) is found effective to meet IEEE 519 standard recommendation on the harmonic level.

Keywords: Adaptive hysteresis band current controller, Compensation reference current signal, Phase lock loop control, Shunt active power filter, Total harmonic distortion.

## 1. Introduction

The rapid increase of industrial infrastructure, which utilizes power electronic devices, increases the non-linear load in power supply network. Various three-phase loads which are nonlinear in nature such as variable frequency drives, thyristor converters, arc furnaces, etc., are accountable for creating the voltage and

**Nomenclatures**

| | |
|---|---|
| $C$ | Capacitance of DC link voltage, $\mu F$ |
| $f_c$ | Average switching frequency, kHz |
| $I_{ca}$ | Actual current of phase A, amp |
| $I^*_{c,a}$ | Current command in phase A, amp |
| ${}^{i}L_a$ | Instantaneous load current of phase A, amp |
| $i_a$, $i_b$, $i_c$ | Compensating current references for all three phases, amp |
| $i_{dc}$ | d-axis compensating current, amp |
| $M$ | Slope of the command current wave |
| $n$ | Harmonic order |
| $V_{ss}$ | The voltage stabilization feedback |
| $v$ | Dc link voltage, volt |
| $v_{sa}$ | Instantaneous phase voltage of grid side bus, volt |

***Greek Symbols***

| | |
|---|---|
| $\theta_1$, $\theta_2$ | Phase angle information of voltage and current from the respective PLLs, deg |
| $\hat{\theta}$ | Output of voltage control oscillator (VCO) |
| $\varphi$ | Phase angle difference between the output current and voltage, deg |

**Abbreviations**

| | |
|---|---|
| ANN | Artificial neural networks |
| APF | Active power filters |
| DSC | Delay signal cancellation |
| EMI | Electromagnetic Interference |
| PCC | Point of common coupling |
| PID | Proportional-Integral-Derivative |
| PLL | Phase-Locked Loops |
| PWM | Pulse width modulation |
| SRF-PLL | Synchronous-Reference-Frame Phase Locked Loop |
| THD | Total harmonic distortion |
| VCO | Voltage control oscillator |
| VSI | Voltage source inverter |

current harmonics in power distribution system and draws large amount of reactive power. Power quality can be improved by suppressing the harmonic pollution and performing reactive power compensation. A great deal of attention has been focused to mitigate it as they overload the utility, cause reliability problems on the equipment such as higher line losses, transformer overheating, machine vibration and a waste of energy [1-3]. The voltage profile of the grid is also distorted because current harmonics in power networks leads to voltage harmonics [3]. The passive harmonic filter has been widely used in industries because of low cost and ease of interfacing. However, with a change in load current the current filtering effect changes and it also leads to series and parallel resonance in the utility network [4-6]. Alternatively, active power filters (APFs) are considered as an effective solution for the above-mentioned problems though they are critical to design and costly in nature [7, 8].

Many research works incorporated active power filters APF, for the elimination of harmonic pollutions and compensation of reactive power in the utility grid [9-11]. The main categories of three-phase, three-wire active power filters are the shunt, series, and hybrid configurations. Their merits and demerits are discussed in [12]. There are many research papers [13, 14] on series APF where a transformer is connected in series to the transmission line to inject the required voltage to filter out the harmonic current. The main disadvantage of series APF is being costly due to the presence of transformer. Series hybrid APF approach proposed by different researchers has the potential for harmonic compensation in high voltage grid with lower APF rating [15].

The instantaneous reactive power theory proposed [16] has been applied earlier for the control of shunt APFs to remove harmonic pollution of grid side current loaded by non-linear load [17]. Artificial neural networks (ANNs) have been applied to various power system problems for extracting the harmonic current to eliminate the harmonics [18-20]. This technique has been successfully applied for making the current perfectly sinusoidal in active power filters and replaces the conventional Proportional-Integral-Derivative (PID) controllers. Hybrid active filter proposed by Peng and Adams, [15] is a combination of active filters and passive filters, to solve the distortion of utility current of power network [21].

The above researches are based on only three-phase balanced voltage with non-linear load. However, in practical application load and source may be unbalanced in nature. For unbalanced condition, if negative sequence current is not extracted, it will be included in reference current command and affect the information of phase angle. This raises the question of the robustness of APFs. Some researchers [22, 23] have used the hysteresis band controller to generate the pulses to trigger the active switches of voltage source inverter which is the heart of APFs. The main drawback of hysteresis band controller is the variable switching frequency, which affects the reliability of operation of voltage source inverter. Adaptive hysteresis band controller proposed in [24, 25] has been successfully used in APFs to make the switching frequency constant.

This paper proposes a new control technique, which takes care of both unbalanced grids and loads side voltage. It also keeps the capacitor voltage constant under different load conditions. In the proposed technique, an adaptive hysteresis band current controller is used to keep the switching frequency constant. The independent estimation of the peak value of load current and the phase angle removes the injection of the negative sequence current in the reference current command generation. The phase angle information is derived from conventional phase lock loop (PLL) controller with normalization and delay signal cancellation (DSC) which separate out the positive and negative sequence.

## 2. Structure of Shunt Active Power Filter

Shunt active power filter is the current controlled voltage source inverter (VSI) powered by a capacitor, connected parallel to the load terminals of the non-linear load. The control technique used to compensate the harmonic injection to the grid current by the non-linear load is called active harmonic filter, otherwise, it is called active power filter if it is used to compensate both harmonic and reactive power. The block diagram of grid connected non-linear load with active power filter at the

point of common coupling (PCC) under study is shown in Fig. 1. In this research work, for generation of the compensating current, a current controlled VSI is used. This compensating current consists of harmonic current and instantaneous reactive current required for the non-linear load. This current is injected to the utility grid to meet the harmonic current and reactive current demands of non-linear load. Thus, the grid provides only the active current demand of the load and keeps the utility current sinusoidal . To generate the compensating current, a reference current signal consisting of both actual harmonic current and reactive component of the non-linear load current is required [26-29]. This paper proposes a new method for reference current generation in which two PLLs are used.

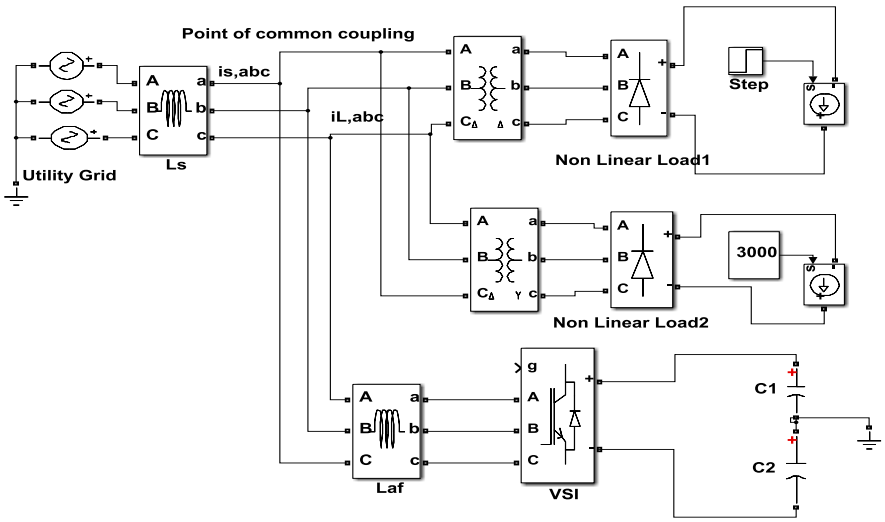


**Fig. 1. Block diagram of active power filter connected to grid with non-linear loads.**

## 3. Proposed Compensation Current Reference Signal Generation Technique

In the proposed method, two PLLs are used to estimate the phase angle information of utility voltage and load current. The cosine of phase angle difference between the output current and voltage PLLs is multiplied with the maximum value of load current signal and sine of the phase angle of the voltage signal to get the instantaneous active current signal. The compensating reference current signal is the difference of load current signal and instantaneous active current signal.

The instantaneous phase voltage of grid side bus is:

$$v_{s,a} = V_m sin\omega t \tag{1}$$

The instantaneous load current of phase A is:

$$i_{L,a} = I_{m1}\sin(\omega t + \varphi_1) + \sum_{n=2}^{\infty} I_{mn}\sin(n\omega t + \varphi_n) \tag{2}$$

Equation (2) can be rewritten as:

$$i_{L,a} = I_{m1} sin\omega t\ cos\varphi_1 + I_{m1} cos\omega t\ sin\varphi_1 + \sum_{n=2}^{\infty} I_{mn}\sin(n\omega t + \varphi_n) \tag{3}$$

The first term, 2nd term and 3rd term of Eq. (3) represent an instantaneous active component, reactive component and harmonics component of current signal respectively.

Let $\omega t = \theta_1$ and $\omega t + \varphi_1 = \theta_2$

Hence,

$$\theta_2 - \theta_1 = \varphi_1 \tag{4}$$

The phase angle information of the voltage $(\theta_1)$ and current $(\theta_2)$ can be estimated through respective PLLs.

The second and third terms of Eq. (3) are used as reference compensating current signal of phase A. Similarly, reference compensating current signal for phase *B* and *C* are derived.

The compensating current references for all phases are:

$$i_a^* = I_{m1} cos\omega t\ sin\varphi_1 + \sum_{n=2}^{\infty} I_{mn} \sin(n\omega t + \varphi_n) \tag{5}$$

$$i_b^* = I_{m1} \cos(\omega t - {}^{2\pi}/_{3})\ sin\varphi_1 + \sum_{n=2}^{\infty} I_{mn} \sin\left(n\omega t + \varphi_n - {}^{2n\pi}/_{3}\right) \tag{6}$$

$$i_c^* = I_{m1} \cos(\omega t + {}^{2\pi}/_{3})\ sin\varphi_1 + \sum_{n=2}^{\infty} I_{mn} \sin\left(n\omega t + \varphi_n + {}^{2n\pi}/_{3}\right) \tag{7}$$

The injection of the current to the grid produced by VSI is made equal to the compensating current reference. The voltage stabilization feedback ($V_{ss}$) signal is added to compensating current reference to keep the capacitor voltage constant. To compensate only the harmonic current and avoiding unit power operation, the second term of compensating current reference should be separated out. This type of control may be called an active harmonic filter. Different types of current control technique can be used to generate the proper gate signals of the inverter to make the grid side current of inverter equal to compensating current reference. Some of the current control methods are instantaneous current control, peak current control, deadbeat control and hysteresis band control. In this paper adaptive hysteresis band, current control technique is used. Switching harmonic current ripple can be partially removed due to the inclusion of inductor in VSI. Control diagram for current command generation and pulses of VSI shown in Fig. 2. Peak current command generation from load current is shown in Fig. 3.

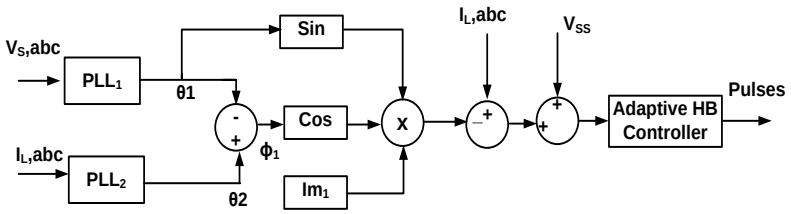


**Fig. 2. Control diagram for current command generation and pulses for VSI.**

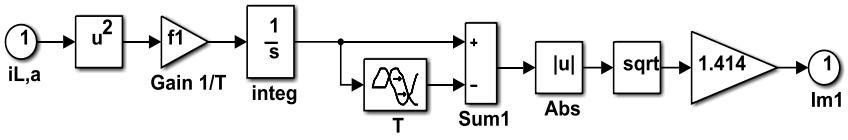


**Fig. 3. Peak current generation from load current.**

## 4. Structure of PLL

Nowadays, the phase angle information of grid voltage and current can be found out by PLL technique. The PLL control technique consists of phase detector, loop filter and voltage control oscillator (VCO). The loop filter consists of PI controller and output of the PI controller is the grid frequency. The accuracy of the phase angle information depends on grid harmonic, notches, frequency disturbances, voltage offset and unbalanced condition. Though this algorithm have a better rejection capability for the above power quality problems on grid compared to zero crossing method, still additional improvements are required, especially for the unbalanced condition. This is because the compensation of harmonic current and reactive power depends on the accuracy of phase angle information. Under the unbalanced condition, the phase angle information is affected by the second order harmonics produced by the negative sequence components, which will merge with the positive sequence current component. To overcome this, the stationary αβ voltages must be free from negative sequence voltages. This is possible by filtering out the negative sequence voltages. There are various methods to separate out positive sequence component current from unbalanced grid voltage. These methods are notch filter, band stop filter and low pass filter [30-32]. This paper uses the modified DSC methods, which not only removes the negative sequence current but also removes the harmonic components of current.

The positive sequence component of unbalanced voltage appears as dc quantity in the DQ-frame rotating in the same direction with grid frequency, while negative sequence voltage appears as 100Hz ac quantity. The multiple of 3rd harmonics appears as 2nd harmonics [33-35]. The (*2n±1*) harmonics appear as *2n* harmonics where *n=2, 3, 4*. This behaviour of harmonics and negative sequence voltage distorts the phase angle information. If the three phase voltages are sinusoidal and balanced then *αβ* voltages are sinusoidal and orthogonal. When the terminal voltages are unbalanced with harmonics, the *αβ* voltages are no longer sinusoidal or orthogonal. Therefore, to get accurate phase angle information, the grid side voltages and load side currents are acquired and the harmonics are filtered out with the help of low pass filter. The outputs of the filter are transformed to αβ frame by the *abc* to *αβ* transformation. To make it orthogonal, the *αβ* voltage should be normalised by the normalisation circuit. The DSC method is used to separate out the positive and negative sequence components. The implementation circuit of the proposed PLL is shown in Fig. 4. Here, first order harmonic filter is used with a cut-off frequency of 60 Hz. The output of the 1st order filter is defined as:

$$v_{\alpha\beta1} = [v_{\alpha1} \quad v_{\beta1}]^T \tag{8}$$

To make $v_{\alpha\beta1}$ orthogonal, the normalising circuit must be used. The normalisation waveforms are:

$$v_{\alpha\beta1}{}^{1} = \frac{1}{\sqrt{(v_{\alpha1})^2+(v_{\beta1})^2}} . v_{\alpha\beta1} \tag{9}$$

The DSC circuit can be used to separate out the positive sequence and negative sequence of normalised waveforms is shown in Fig. 5.

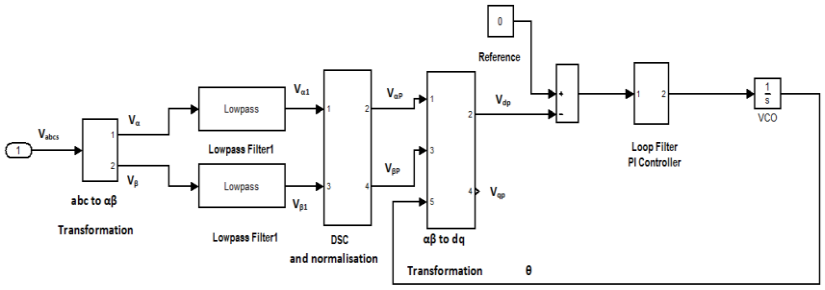


**Fig. 4. Structure of PLL.**

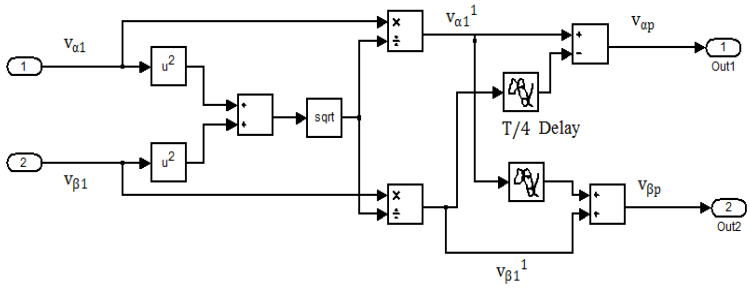


**Fig. 5. Separation of +ve sequence from distorted signal through normalisation and delay signal cancellation.**

The mathematical expressions are:

$$\widehat{v_{\alpha p}} = \frac{1}{2}[v_{\alpha1}{}^{1} - v_{\beta1,del}{}^{1}] \tag{10}$$

$$\widehat{v_{\beta p}} = \frac{1}{2}[v_{\beta1}{}^{1} + v_{\alpha1,del}{}^{1}] \tag{11}$$

$$\widehat{v_{\alpha n}} = \frac{1}{2}[v_{\alpha1}{}^{1} + v_{\beta1,del}{}^{1}] \tag{12}$$

$$\widehat{v_{\beta n}} = \frac{1}{2}[v_{\beta1}{}^{1} - v_{\alpha1,del}{}^{1}] \tag{13}$$

where $[v_{\alpha1,del}{}^{1}\ v_{\beta1,del}{}^{1}] = [v_{\alpha1}{}^{1}\left(t-\frac{T}{4}\right)\ v_{\beta1}{}^{1}\left(t-\frac{T}{4}\right)]$ and subscripts $p$ and $n$ stands for positive and negative sequence respectively. $T$ is the period of the signal. The signals ($\widehat{v_{\alpha p}}$ , $\widehat{v_{\beta p}}$) from DSC is transferred to synchronous reference ($dq$) by using unit vector, which is represented as:

$$T_e(\hat{\theta}) = \begin{pmatrix} cos\hat{\theta} & -sin\hat{\theta} \\ sin\hat{\theta} & cos\hat{\theta} \end{pmatrix} \quad (14)$$

where $\hat{\theta}$ is the output of VCO.

## 5. Stabilisation of DC Link Capacitor Voltage

It is necessary to keep the DC link voltage across the capacitor to be constant and equal to the reference command value under sudden disturbances of the load. To achieve this closed-loop control technique must be required. This technique will provide the best result if it will get associated with a proportional-integral (PI) controller which posses satisfactory behaviour for regulation of DC variables.

The mathematical model of the DC link dynamics can be found out by considering the input-output power balance for active VSI under no load condition.

The governing equations are:

$$\frac{3}{2}\left(v_d i_{dc} + v_q i_{qc}\right) = C v_0 \frac{dv_0}{dt} \quad (15)$$

The small signal analysis of the above for linearization leads to:

$$\frac{3}{2}\left\{(V_d + \widehat{v_d})(I_{dc} + \widehat{i_{dc}}) + (V_q + \widehat{v_q})(I_{qc} + \widehat{i_{qc}})\right\} = C(V_0 + \widehat{v_0})\frac{d(V_0 + \widehat{v_0})}{dt} \quad (16)$$

So here, the dc link voltage $v_0$ can be controlled through the d-axis compensating current $i_{dc}$ and therefore other perturbation can be considered to be null.

Neglecting second order signal perturbations and $\frac{3}{2}\left(V_d I_{dc} + V_q I_{qc}\right) = C V_0 \frac{dV_0}{dt}$, leads to:

$$\frac{3}{2} V_d \widehat{i_{dc}} = C V_0 \frac{d\widehat{v_0}}{dt} \quad (17)$$

Thus the transfer function is:

$$\frac{\widehat{v_0}(S)}{\widehat{i_{dc}}(S)} = \frac{3V_d}{2CSV_0} \quad (18)$$

Based on the above transfer function the PI controller can be designed for the DC voltage loop. It must have sufficiently lower band width with respect to hysteresis band controller so as to have a proper decoupling. The closed-loop block diagram is shown in Fig. 6.

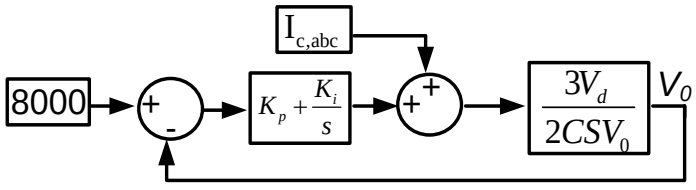


**Fig. 6. Voltage stabilisation circuit.**

## 6. Adaptive Hysteresis Band Current Controller

Among all PWM techniques [36, 37], the hysteresis band controller has been popularly used in various applications to control the flow of current in a limited bandwidth as per command current value. This is because of fast response, easy implementation, inherent peak current limiting capabilities, unconditional stability and good accuracy. However, the basic hysteresis band controller suffers due to the large variation of switching frequency. The switching frequency of hysteresis band controller depends on system mathematical equations at each instant and band width of hysteresis band controller. This demands the band width should be adopted at every instant in order to keep the switching frequency constant. The band width of hysteresis band controller is adopted depending upon the rate of rising and rate of fall of controlled current as proposed by Bose [24]. This paper uses the same analysis to adapt the bandwidth of hysteresis band controller for removing the harmonics and compensation of reactive power from the utility, connected with the non-linear load.

The conventional hysteresis band controller is shown in Fig. 7, composed of hysteresis around the current command signal. Let the current command in phase a is denoted as $I_{ca}^{*}$ and the actual current of phase a on ac side of the voltage source inverter is $I_{ca}$.The switching pattern for phase a of VSI can be described as:

If $i_{ca} < (i_{ca}^{*} - HB)$ ; upper switch is ON and lower switch is OFF for leg a

and $i_{ca} > (i_{ca}^{*} - HB)$; upper switch is OFF and lower switch is ON for leg a

Similarly, other two legs, switching pattern can be determined. Since the width of hysteresis controller is constant, the switching frequency operation in VSI is uneven. This creates problems such as designing the filter, noise formation, Electromagnetic Interference (EMI) problem and failure of operation of the active switch due to the very high switching frequency, which is beyond the capacity of the switch. By changing the bandwidth at every instant, the average switching frequency is made to be constant, which nullify the above-mentioned problems.

Figure 7 shows the falling and rising of current inside the band to generate the pulses for operation of VSI. The equation can be written as:

$$\frac{di_{ca}^{+}}{dt} = \frac{1}{L}(0.5V_0 - v_s) \qquad 0 < t < t1 \tag{19}$$

$$\frac{di_{ca}^{-}}{dt} = \frac{1}{L}(0.5V_0 + v_s) \qquad t1 < t < t2 \tag{20}$$

From the geometry of Fig. 7, the equations can be written as:

$$t1\left(\frac{di_{ca}^{+}}{dt} - \frac{di_{ca}^{*}}{dt}\right) = 2HB \tag{21}$$

$$t2\left(\frac{di_{ca}^{-}}{dt} - \frac{di_{ca}^{*}}{dt}\right) = -2HB \tag{22}$$

$$t1 + t2 = \frac{1}{f_c} \tag{23}$$

On simplifying the equations, the bandwidth becomes

$$HB = \frac{V_0}{8Lf_c}\left[1 - \frac{4L^2}{V_0^2}\left(\frac{v_S}{L} + m\right)^2\right] \quad (24)$$

where $f_c$ is the average switching frequency and $m = \frac{di_{ca}^*}{dt}$ is the slope of the command current wave.

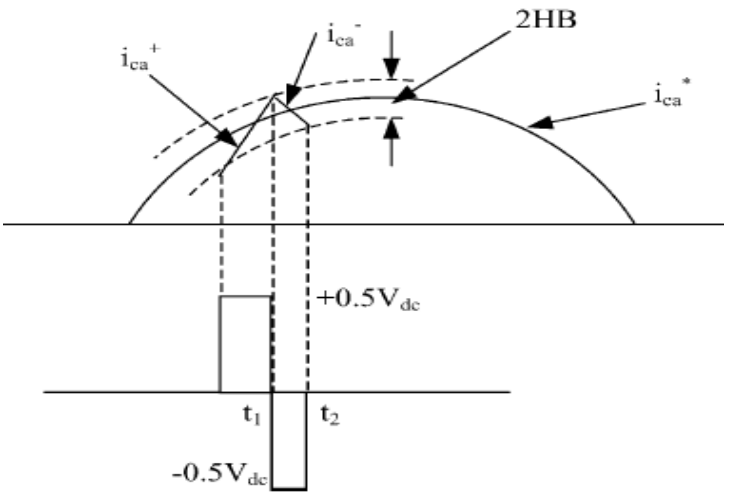


**Fig. 7. Voltage and current envelopes with hysteresis band current control for active power filters (APF).**

The implementation of adaptive hysteresis band controller for pulse generation in MATLAB simulink is shown in Fig. 8.

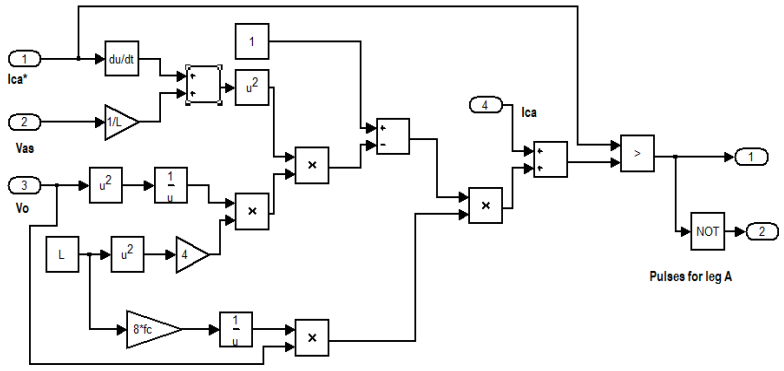


**Fig. 8. Implementation of adaptive hysteresis band controller.**

## 7. Results and Discussion

The circuit used for simulation consists of utility grid of phase voltage 4160 V with source inductance of 100 mH and a non-linear load. A load current of 6000. A flow through the two-diode rectifiers, connected via two isolation 1:1 Delta-Delta and

Delta-Star transformers. The Delta-Star rectifier is connected after 10 cycles to increase the load current from 3000A to 6000A. The load draws the reactive power from the utility grid and injects the harmonics, which distorts the grid side current ($I_s$). According to IEC standard-50, the grid should not have a total harmonic distortion larger than 5% [38]. The distortion limit for all odd harmonics is given in Table 1. To compensate for the reactive power and to mitigate the harmonics, a shunt APF is used. The design specification and circuit parameters used in the simulation are indicated in Table 2.

**Table 1. Distortion limits for distributed generation system set by IEC standard-50.**

| Odd harmonics | Distortion limit |
|---|---|
| $3^{rd}$ -$9^{th}$ | < 4% |
| $11^{th}$ -$15^{th}$ | < 2% |
| $17^{th}$ -$21^{st}$ | < 1.5% |
| $23^{rd}$ -$33^{rd}$ | < 0.6% |

**Table 2. Design specification and parameters (to be specific).**

| | |
|---|---|
| Switching frequency | 10 kHz |
| Grid frequency | 60 Hz |
| Grid phase voltage(rms) | 4160 V |
| Transmission inductance | 100 mH |
| Load current | 3000A-6000 A |
| DC link Voltage across capacitor | 8000 V |
| Inverter side inductance | 1 mH |
| Capacitor value | 500 µF |

As per the proposed algorithms, the current command generation for compensation of reactive power and elimination of harmonics is shown in Fig. 9. The actual current generated through VSI using adaptive hysteresis band controller, which is injected to the utility grid at PCC, is shown in current command Fig. 9 for comparison. It demonstrates that actual current can keep track of the current command. The source current before and after the compensation is illustrated in Fig. 10. A comparison is made not only for single load but also for different loads by operating another diode bridge rectifier load after 10 cycles. The reactive power flows before and after compensation shown in Fig. 11 illustrates the reactive power compensation capability of APF for different load conditions.

Due to capacitor voltage, feedback the voltage across the capacitor is held constant through the load is increased. It is illustrated in Fig. 12. The total harmonic distortion (THD) is computed in the source current for one rectifier and two rectifiers in operations as shown in Fig. 13. For one rectifier with a load current of 3000 A, the THD of source current is 20.57% before compensation, whereas the THD of source current is 2.26 % after compensation, which is far below than IEEE-519. For both rectifiers with a current load of 6000 A, the THD of source current before compensation is 4.81%, which remains within the harmonic standard limit of IEEE-519 [39]. It is changed to 1.55% after compensation. However, THD is lying less than IEEE-519 standard, reactive power compensation may be required in two-diode rectifier's load, which demands active power filter. The THDs with respect to fundamental for different load condition before and after compensations are shown in Fig. 13.

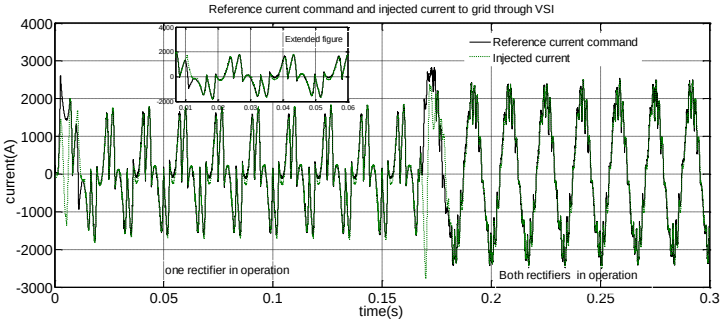


**Fig. 9. Reference current command and injected current to grid through VSI.**

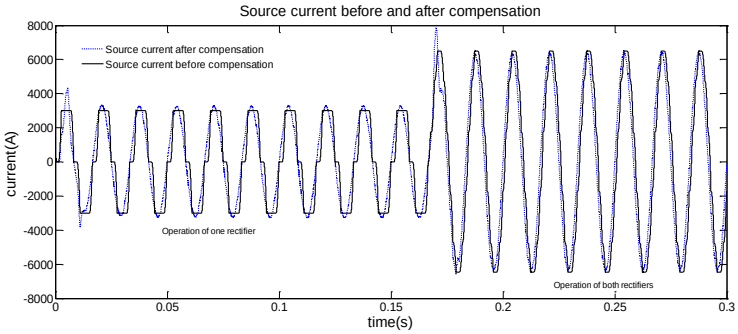


**Fig. 10. Source current before and after compensation.**

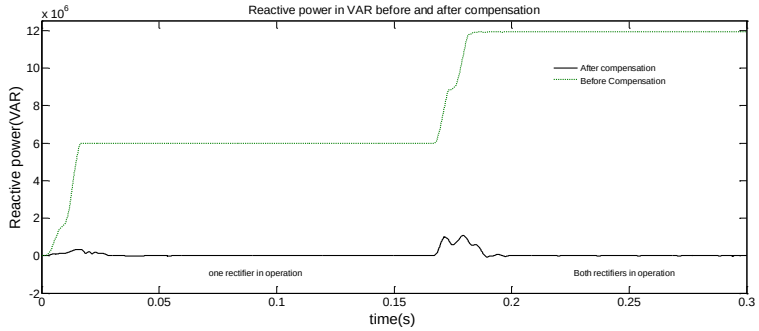


**Fig. 11. Reactive power flow from grid before and after compensation.**

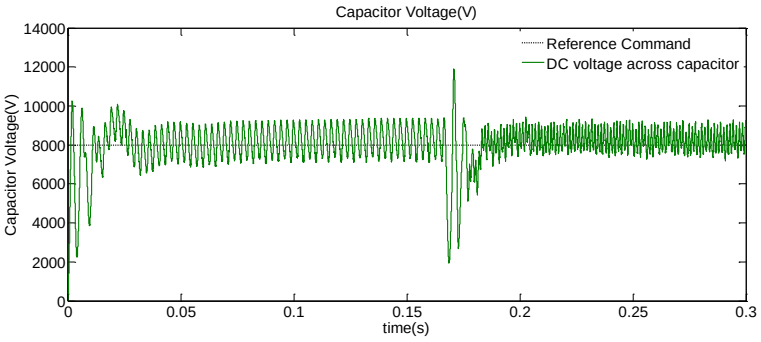


**Fig. 12. Capacitor voltage under different loaded conditions.**

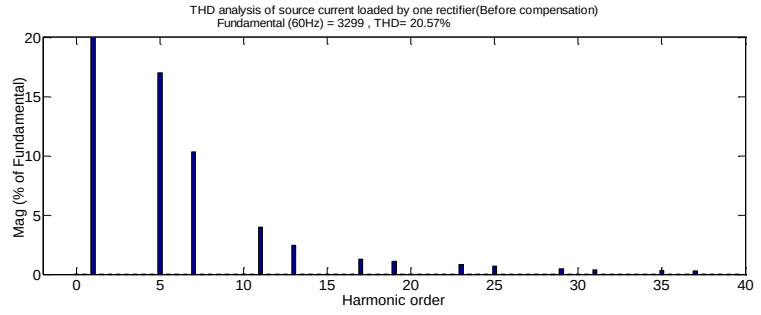


**(a)**

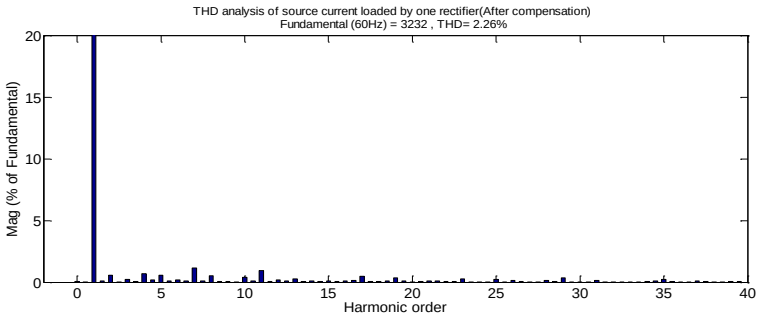


**(b)**

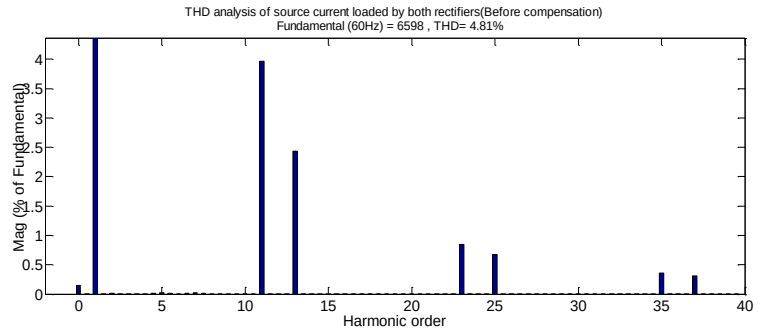


**(c)**

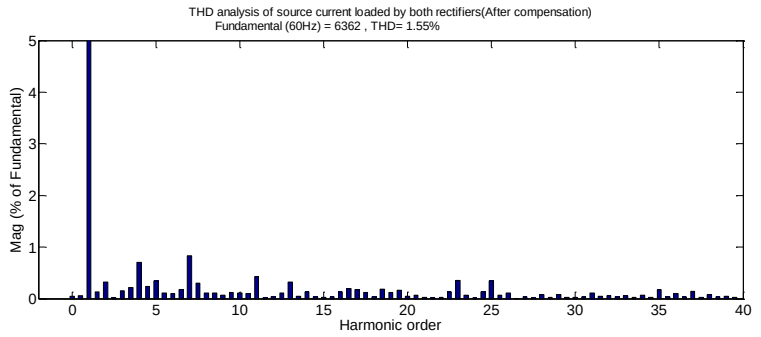


**(d)**

**Fig. 13. THD analysis of source current (a) before compensation with one rectifier (b) after compensation with one rectifier (c) before compensation with two rectifiers (d) after compensation with two rectifiers in operation.**

## 8. Conclusions

This work describes the validity of the proposed reference current command generation technique for injecting current to the utility grid through VSI, which is used for compensation of reactive power and harmonics. In the proposed work through two PLLs are used, the control structure is simple and straightforward. The structure of PLLs for getting the information of phase angles of the source voltage and load current is designed and made robust under distorted conditions. The voltage profile of capacitor is kept constant throughout the operation with the different load by providing a voltage feedback signal to reference current command. The dynamics of voltage feedback is explained in detail. Adaptive hysteresis band controller explained in [24], has a bandwidth, which is programmed as a function of system parameters to keep the switching frequency fairly constant is implemented here in order to optimise the PWM performance.

The simulation study results of the proposed APF are found suitable not only for single load current but also for the different level of load current for the elimination of the harmonics and compensation of the reactive power from utility current. The simulation study shows that it is effective for harmonic elimination and keeps the THD level well within the IEEE standard for different types of non-linear load. The study also reveals that the injection of reactive power to the utility through VSI is accurately controlled to operate the grid at unity power factor. The validity of the proposed control technique was effectively proved through simulation results only. Experimental verification of the proposed technique is being carried out and test results will be reported in the future papers.

## References

1. Turunen, J.; Salo, M.; and Tussa, H. (2005). Comparison of series hybrid active power filters based on experimental tests. *Proceedings of the European Conference of Power Electron Application*. Dresden, Germany, 10 pages.
2. Abdalla, I.I.; Rao, K.S.R.; and Perumal, N. (2011). Three-phase four-leg shunt active power filter to compensate harmonics and reactive power. *Proceedings of the Symposium on Computers and Informatics,* Kuala Lumpur, Malaysia, 495-500.
3. Grady, W.M.; Samotyj, M.J.; and Noyola, A.H. (1990). Survey of active power line conditioning methodologies. *IEEE Transactions on Power Delivery*, 5(3), 1536-1542.
4. Karshenas, H.R.; and Saghafi, H. (2006). Basic criteria in designing LCL filters for grid connected converters. *Proceedings of the IEEE International Symposium on Industrial Electronics*. Montreal, Canada, 1996-2000.
5. Liserre, M.; Blaabjerg, F.; and Hansen, S. (2005). Design and control of an lcl-filter-based three-phase active rectifier. *IEEE Transactions on Industry Applications*, 41(5), 1281-1291.
6. Zeng, G.; Rasmussen, T.W.; and Teodorescu, R. (2010). Design and control of LCL-filter with active damping for active power filter. *IEEE International Symposium on Industrial Electronics.* Bari, Italy, 2557-2562.
7. Komatsu, Y.; and Kawabata, T. (2018). A control method for the active power filter in unsymmetrical and distorted voltage systems. *Proceedings of the Power Conversion Conference.* Nagaoka, Japan, 1249-1260.

8. Xiao, P.; Venayagamoorthy, G.K., Corzine, K.A. (2009). Seven-level shunt active power filter for high-power drive systems. *IEEE Transactions on Power Electronics*, 24(1), 6-13.
9. Panigrahi, R.; Subudhi, B.; and Panda, P.C. (2016). A robust LQG servo control strategy of shunt-active power filter for power quality enhancement. *IEEE Transactions on Power Electronics*, 31(4), 2860-2869.
10. Yousfi, A.; Allaoui, T; and Chaker, A. (2016). Five-level shunt active filter based on instantaneous p-q theory and fuzzy logic controller connected to a photovoltaic source. *Journal of Electrical Engineering*, 16(3), 1-8.
11. El-Habrouk, M.; Darwish, M.K.; & Mehta, P. (2000). Active power filters: A review. *IEE Proceedings-Electric and Power Application*, 147(5), 403-413.
12. Salam, Z.; Tan, P.; and Jusoh, A. (2006). Harmonics mitigation using active power filter: A technological review. *Elektrika*, 8(2), 17-26.
13. Dixon, J.W.; Venegas, G.; and Moran, L.A. (1997). A series active power filter based on a sinusoidal current-controlled voltage-source inverter. *IEEE Transactions on Industrial Electronics*, 44(5), 612-620.
14. Lee, G.-M.; Lee, D.-C.; and Seok, J.-K. (2004). Control of series active power filters compensating for source voltage unbalance and current harmonics. *IEEE Transactions on Industrial Electronics*, 51(1), 132-139.
15. Peng, F.Z.; & Adams, D.J. (1999). Harmonic sources and filtering approaches-series/parallel, active/passive, and their combined power filters. *Proceedings of the IEEE Industry Applications Conference*. Phoenix, United States of America, 448-455.
16. Akagi, H.; Kanazawa, Y.; and Nabae, A. (1984). Instantaneous reactive power compensators comprising switching devices without energy storage components. *IEEE Transactions on Industry Applications*, IA-20(3), 625-630.
17. Akagi, H.; Watanabe, E.; and Aredes, M. (2007). *Instantaneous power theory and applications to power conditioning.* Hoboken, New Jersey: John Wiley & Sons.
18. Bose, B.K. (2007). Neural network applications in power electronics and motor drives-an introduction and perspective. *IEEE Transactions on Industrial Electronics*, 54(1), 14-33.
19. Widrow, B.; and Plett, G.L. (1997). Nonlinear adaptive inverse control. Proceedings *of the 36th IEEE Conference on Decision and Control*. San Diego, United States of America, 1032-1037.
20. Haykin, S.O. (2009). *Neural networks and learning machines.* Pearson Education.
21. Blaabjerg, F.; Teodorescu, R.; Liserre, M.; and Timbus, A.V (2006). Overview of control and grid synchronization for distributed power generation systems. *IEEE Transactions on Industrial Electronics*, 53(5), 1398-1409.
22. Oh, D.S.; and Youn, M.J. (1990). Automated adaptive hysteresis current control technique for a voltage-fed PWM inverter. *IET Electronics Letters*, 26(24), 2044-2046.
23. Rahman, K.M.; Khan, M.R.; Choudhury, M.A.; and Rahman, M.A. (1997). Variable-band hysteresis current controllers for PWM voltage source inverters. *IEEE Transactions on Power Electronics.* 12(6), 964-970.

24. Bose, B.K. (1990). An adaptive hysteresis-band current control technique of a voltage-fed pwm inverter for machine drive system. *IEEE Transactions on Industrial Electronics*, 37(5), 402-408.
25. Kale, M.; and Ozdemir, E. (2005). An adaptive hysteresis band current controller for shunt active power filter. *Electric Power System Research*, 73(2), 113-119.
26. Svensson, J. (2001). Synchronisation methods for grid-connected voltage source converters. *IEEE Proceedings - Generations, Transmission, Distribution*, 148(3), 229-235.
27. Klumpner, C.; Liserre, M.; and Blaabjerg, F. (2004). Improved control of an active-front-end adjustable speed drive with a small dc-link capacitor under real grid conditions. Proceedings of the *IEEE 35th Annual Power Electronics Specialists Conference. Achen, Germany*, 1156-1162.
28. Buso, S.; Malesani, L.; and Mattavelli, P. (1998). Comparison of current control techniques for active filter applications. *IEEE Transactions on Industrial Electronics*, 45(5), 722-729.
29. Singh, B., Al-Haddad, K., and Chandra, A. (1998). A new control approach to three-phase activity: filter for harmonics and reactive power compensation. *IEEE Transactions on Power Systems*, 13(1), 133-138.
30. Rao D.B; and Kung, S.-Y. (1984). Adaptive notch filtering for the retrieval of sinusoids in noise. *IEEE Transactions on Acoustics, Speech and Signal Processing*, 32(4), 791-802.
31. Roncero-Sanchez, P.; Garcia, X.d.T.; Torres, A.P.; and Feliu, V. (2013). Fundamental positive- and negative- sequence estimator for grid synchronization under highly disturbed operating conditions. *IEEE Transactions on Power Electronics*, 28(8), 3733-3746.
32. Schaumann R.; Xiao, H.; and Valkenburg, M.V. (2001). *Design of analog filters*. 2nd edition. New York: Oxford University Press.
33. Hsieh, G.-C.; and Hung, J.C. (1996). Phase-locked loop techniques. A survey. *IEEE Transactions on Industrial Electronics*, 43(6), 609-615.
34. Kaura, V.; and Blasko, V. (1997). Operation of a phase locked loop system under distorted utility conditions. *IEEE Transactions on Industrial Applications*, 33(1), 58-63.
35. Chung, S.-K. (2000). A phase tracking system for three phase utility interface inverters. *IEEE Transactions on Power Electronics*. 15(3) 431-438.
36. Patel, M.A.; Patel, A.R.; Vyas, D.R. and Patel, K.M. (2009). Use of PWM techniques for power quality improvement. *International Journal of Recent Trends in Engineering*, 1(4), 99-102.
37. Chen, D.; and Xie, S. (2004). Review of the control strategies applied to active power filters. *Proceedings of the IEEE International Conference on Electric* Ulitity *Deregulation, Restructuring and Power Technologies.* Hong Kong, China, 666- 670.
38. Teodorescu, R.; Liserre, M.; and Rodriguez, P. (2011). *Grid converters for photovoltaic and wind power system*. West Sussex: John Wiley and Sons.
39. IEEE Standard. (2003). *Standard for interconnecting distributed resources with electric power systems.* New York: The Institute of Electrical and Electronics Engineers, Inc.